Article

# Interpretation of Temperature Control for Ternary Distillation

Min-Te Lin, Cheng-Ching Yu, and Michael L. Luyben

*Ind. Eng. Chem. Res.*, **2005**, 44 (22), 8277-8290 • DOI: 10.1021/ie050130m

# Interpretation of Temperature Control for Ternary Distillation

**Min-Te Lin,[†] Cheng-Ching Yu,[*,†] and Michael L. Luyben[‡]**

*Department of Chemical Engineering, National Taiwan University, Taipei 106-17, Taiwan, and E. I. du Pont de Nemours & Co., Inc., 1007 Market St. - B7434, Wilmington, Delaware 19898*

Even with recent advances in technology for on-line composition measurement, temperature remains the dominant control configuration in distillation columns for product purity. In controlling industrial ternary distillation columns, with a nonmonotonic composition profile for the intermediate boiler, significantly different closed-loop composition dynamics are observed when the temperature-control tray is above or below the intermediate boiler composition turning point (i.e., above or below the tray where the intermediate exhibits a maximum). In this work, the role of direct temperature control is interpreted in the composition space. First, the temperature isotherm is established in the triangular composition space and the process direction and control direction can be clearly distinguished. Then, a quantitative measure, called the traveling distance, for all tray compositions under a specific temperature-control configuration is defined. The traveling distance can be computed directly from process and load transfer function matrices. Rigorous nonlinear distillation column simulations confirm that a temperature-control point with a large traveling distance results in slow composition dynamics (e.g., considering the tray composition can be changed with a fixed rate) and, consequently, poorer control performance. The situation with the difference in traveling distance can become worse when two temperatures are controlled in the column. Finally, this concept is extended to direct composition control of ternary distillation systems. The results clearly show that improved temperature or composition control can be achieved by avoiding a potential conflict in the process and control directions.

## 1. Introduction

Distillation remains the dominant separation technology in many industrial processes. The control of distillation columns has been the subject of much work over the decades that continues today as new problems and challenges emerge. For simple column configurations (one feed, no intermediate heat sources or sinks, and two product streams), we have six degrees of freedom available for manipulation (feed flow, reboiler duty, bottoms flow, condenser duty, reflux flow, and distillate flow). We also have three inventory variables that must be controlled within some range (pressure, reflux drum level, and base level). Feed flow is typically set by the unit upstream of the column. This leaves two degrees of freedom available for controlling column product composition.

The design basis for columns typically involves specifying certain purities or component recoveries in one or two product streams. The achievement of the design objectives depends on the performance of the column controls. In principle, we would like to have direct, instantaneous on-line measurement of product purities. Many advances have been made in technology for on-line composition measurement. But we still have many systems where such measurements do not exist, are too hazardous, are not feasible, are not maintained adequately, are too slow, are too expensive, etc. Hence, column temperatures are still the main controlled variable in distillation columns for product purity control.

Temperature control of distillation columns has been the subject of numerous papers over the last 50 years. Rademaker et al.[1] present a good summary of the various ideas and criteria generated over the years. Buckley et al.[2] discuss various approaches for indirect composition control, which include differential temperature, pressure-compensated temperature, double-differential temperature, and average temperature. Most of the temperature selection criteria are based on the sensitivity with respect to input or load changes. Downs and Moore[3] propose a multivariable version using the singular value decomposition (SVD). Following in the same vein, the nonsquare relative gain (NRG) by Chang and Yu[4] and Cao and Rossiter[5] is also effective in screening possible temperature-control trays. Another approach to indirect composition control is to estimate composition from temperature measurements. This work includes heuristic-based modeling,[6] least-squares-based modeling,[7] and partial least-squares-based modeling.[8−11] The above-mentioned approaches may provide effective temperature control, but the explanation behind the success or failure of different temperature-control points is rarely addressed, particularly for multicomponent systems.

The motivation for this work comes from experience on an actual industrial distillation column.[12] This column effectively separates 3 components and has ∼32 theoretical stages with the temperature profile shown in Figure 1. When we choose a temperature-control

* Corresponding author. Tel.: +886-2-3365-1759. Fax: +886-2-3366-3037. E-mail: ccyu@ntu.edu.tw.
[†] National Taiwan University.
[‡] E. I. du Pont de Nemours & Co., Inc.

10.1021/ie050130m CCC: $30.25 
Published on Web 09/27/2005

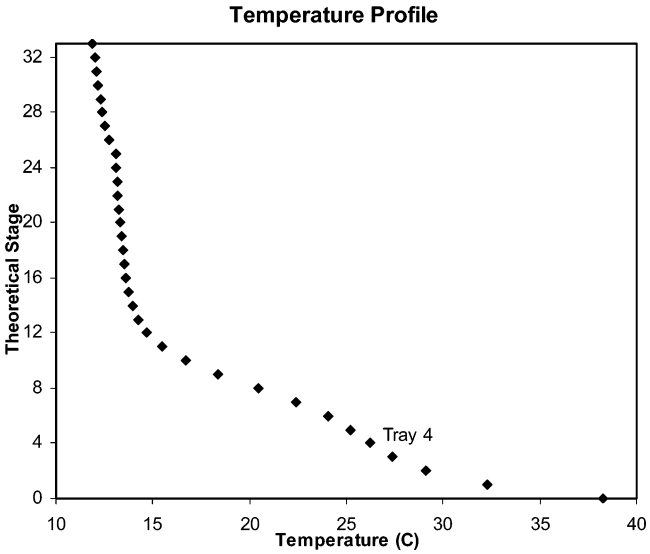


**Figure 1.** Industrial column temperature profile.

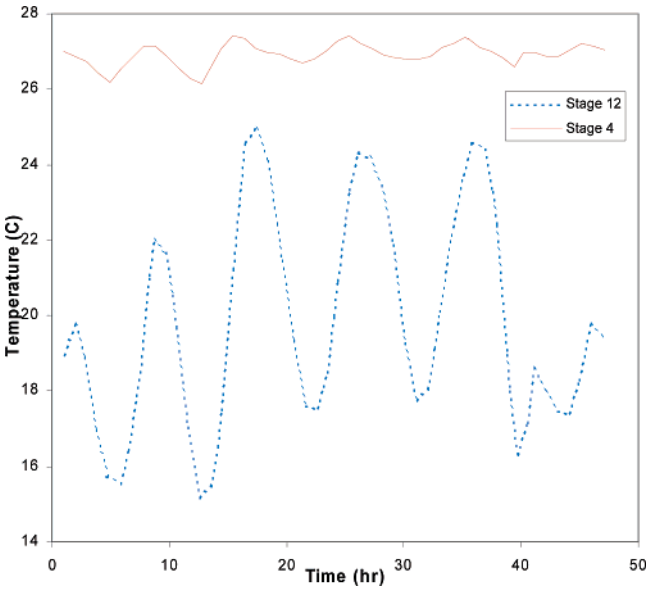


**Figure 2.** Cycling in column temperatures.

location, we typically look for a point where the temperature changes significantly over a few trays. This tends to indicate a break in the composition profile of a component and means that the temperature will be sensitive to a manipulator (e.g., reflux flow or reboiler duty). We do not want to choose a temperature that is in a flat zone, since it will not be sensitive to changes in column conditions.

In the industrial column, theoretical stage 4 (from bottom) was historically used *for decades* as the temperature-control location with reboiler steam flow as the manipulator. This seems to be a reasonable choice when looking at the temperature profile. However, whenever the column experienced a significant change in the feed composition of the intermediate component, the temperatures above stage 4 would undergo cycles of much greater magnitude than what was seen on stage 4. Figure 2 shows some actual column data where stage 4 temperature is being controlled within ~1 °C while the stage 12 temperature cycles by over 4 °C. A study on this column showed that this behavior arose from the

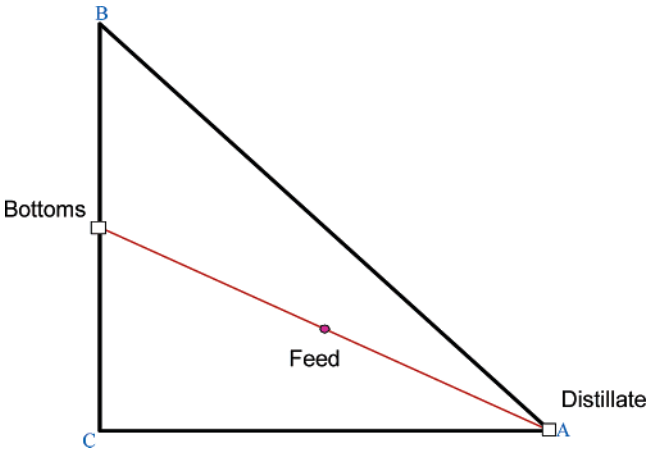


**Figure 3.** Triangular composition space for direct separation with material balance line.

**Table 1. Steady-State Operating Conditions**

| | |
|---|---|
| column feed flow rate ($F$) | 100.0 (lbmol/h) |
| reflux flow rate ($R$) | 109.222 (lbmol/h) |
| distillate flow rate ($D$) | 50.848 (lbmol/h) |
| reflux ratio (RR) | 2.148 (mole fraction) |
| bottom flow rate ($B$) | 49.152 (lbmol/h) |
| vapor boilup ($V$) | 160.169 (lbmol/h) |
| no. of trays (NT) | 25 |
| feed tray (NF) | 18 |
| relative volatilities ($\alpha_A/\alpha_B/\alpha_C$) | 4/2/1 |
| hydraulic time constant ($\beta$) | 3.2 (s) |
| bottom holdup ($M_B$) | 17.435 (lbmol) |
| reflux holdup ($M_D$) | 13.339 (lbmol) |
| tray holdup ($M_N$) | 0.592 (lbmol) |
| feed composition ($Z_A/Z_B/Z_C$) | 0.5/0.2564/0.2436 (mole frac) |
| distillate composition ($x_{D,A}/x_{D,B}/x_{D,C}$) | 0.982/1.75E−2/5E−4 (mole frac) |
| bottom composition ($x_{B,A}/x_{B,B}/x_{B,C}$) | 0.001/0.503/0.496 (mole frac) |
| Antoine vapor pressure coefficient ($A_A/A_B/A_C/B$) | 15.2/14.51/13.8/−2768.55 |
| normal boiling point ($T_A$, $T_B$, $T_C$) | 323.15, 351.6, 385.54 (K) |

composition profile of the intermediate-boiling component and that it mattered whether the temperature-control location is chosen above or below the tray where the intermediate boiler exhibits a maximum.

This paper studies the problem of temperature control for a generic ternary distillation column. We focus on a ternary mixture since multicomponent columns can often be simplified down to three-component systems. We interpret the temperature profile in composition space and define a quantitative measure, called the traveling distance, to explain why we want to select a temperature-control location on the correct side of the intermediate-boiling component profile maximum.

## 2. Interaction between Temperature and Composition

**2.1. Process Description.** We consider as an example a three-component (A, B, and C) separation assuming the following constant relative volatilities:

$$\alpha_A/\alpha_B/\alpha_C = 4/2/1$$

Figure 3 shows in triangular composition space the direct separation process where component A is removed overhead and components B and C are removed in the bottoms. Table 1 contains the steady-state column process conditions for a design with 25 theoretical stages. We have assumed certain vapor pressure coefficients in an Antoine-type correlation to translate from

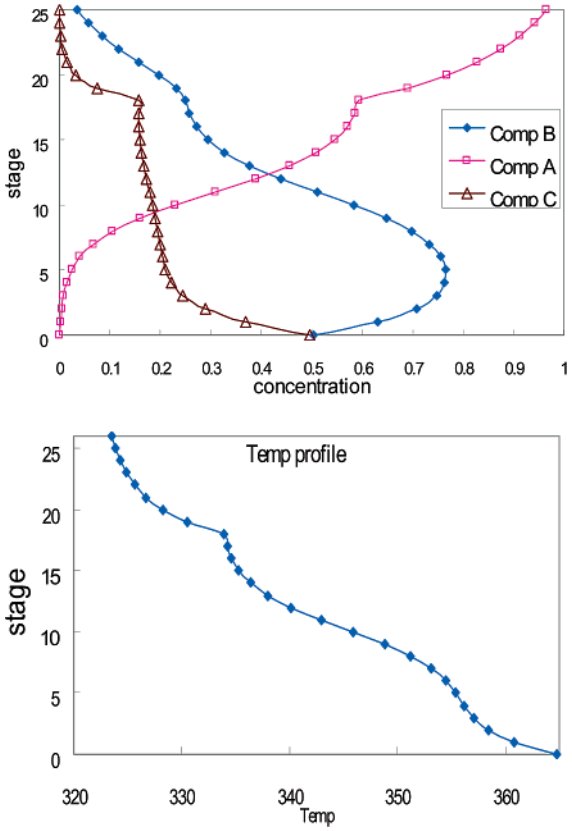


**Figure 4.** Composition and temperature profile for the system studied.

the composition space to a temperature profile. Figure 4 shows the composition and temperature profiles for the column. The key feature to note is the behavior of the intermediate boiler (component B). As we go down the column, the composition of B increases until we reach a maximum of ~0.8 mole fraction at about theoretical stage 5; then the composition decreases and is only 0.5 mole fraction in the bottoms product. This nonmonotonic composition profile exists in all ternary distillation columns, making them unique from binary separations, for both ideal and nonideal components. Where we want to choose the temperature-control point is governed by the location of this maximum. For the ideal distillation system with the equal molar overflow assumption, the relationship between temperature and composition can be described by the bubble point temperature equation:

$$P = \Sigma x_i P_i^{\text{sat}} = x_A \exp\left(A_A + \frac{B}{T}\right) + x_B \exp\left(A_B + \frac{B}{T}\right) + x_C \exp\left(A_C + \frac{B}{T}\right)$$

Note that the Antoine coefficient $B$ is constant for the ideal system. $P$ is the column pressure, and $T$ is temperature. Rearranging the equation, the temperature can be obtained directly given the liquid-phase composition.

$$T = \frac{B}{\ln \frac{P}{x_A \exp(A_A) + x_B \exp(A_B) + x_C \exp(A_C)}}$$

**2.2. Temperature Control and Observations.** If we consider typical load disturbances for the column,

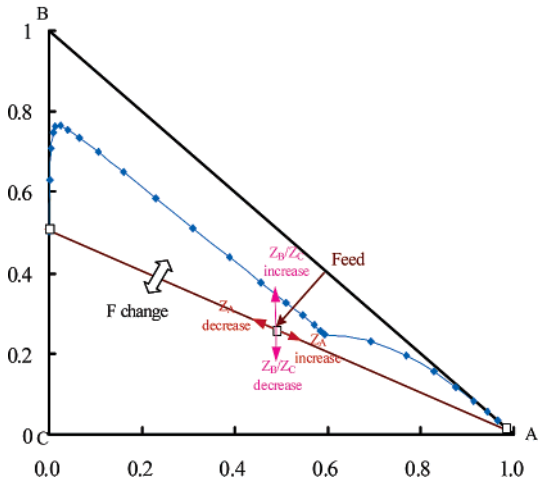


**Figure 5.** Nominal column composition profile, material balance line, and effects of load disturbances on the feed location ($Z_A$ and $Z_B/Z_C$ changes) and material balance line ($F$ change).

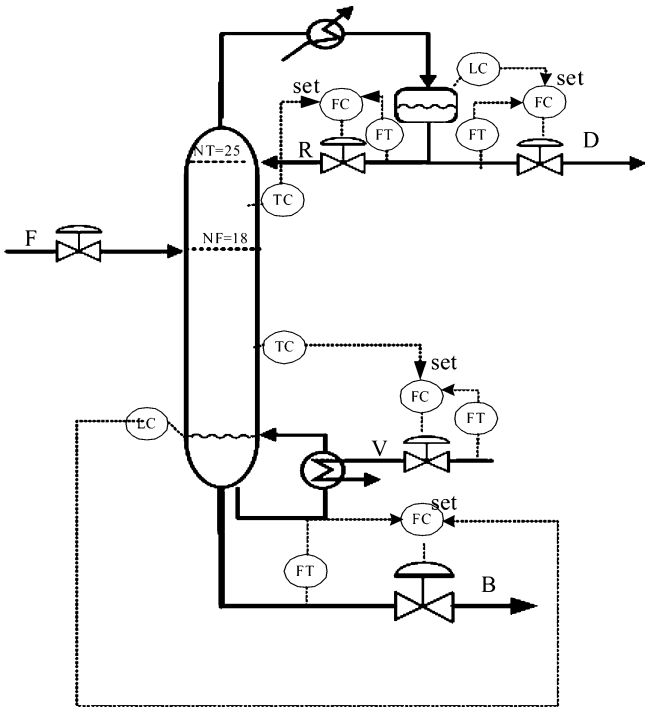


**Figure 6.** Dual-end temperature control with R−V control structure.

we can visualize how they affect the column in composition space (Figure 5). Changes in the feed composition of A, $Z_A$, will move along the direction of the straight line connecting the distillate and bottoms compositions. Changes in the ratio of the feed compositions of B and C, $Z_B/Z_C$, will move the process along a vertical direction. Changes in the feed flow will either stretch/compress the end points of the material balance line or rotate the material balance line using the feed point as the origin or pivot. The particular open-loop behavior depends on the chosen control structure (e.g., fixing reflux−vapor rate or distillate−vapor rate).

A standard dual-composition control strategy is shown in Figure 6. We use reflux to control a temperature toward the top of the column and reboiler duty to control a temperature toward the bottom of the column. This is called the R−V strategy. Many columns operate with

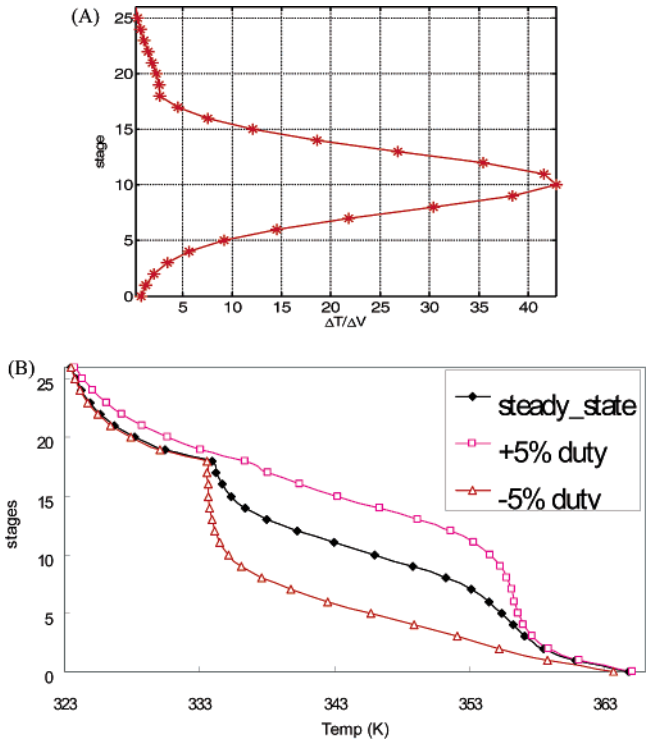


**Figure 7.** (A) Temperature sensitivity for ±0.001% change in boilup rate and (B) temperature profile for ±5% change in boilup rate.

only single-end control that uses one temperature. Since vapor boilup has a fast and significant effect on column temperatures, it often is the manipulator of choice. We need to determine which temperature to use for control. The two common requirements in picking a good temperature-control location are (1) we want the manipulator to have a significant effect on the temperature (ratio of temperature change to manipulator change is large) and (2) we want the response to be somewhat symmetric (an increase or decrease in manipulator causes about the same relative effect). Figure 7A shows the sensitivity analysis of the temperature profile to a 0.001% change in vapor boilup. If we look at possible temperature-control trays, $T_1$ is somewhat related to the bottoms-product composition but it does not have a large gain, $T_5$ is the tray location giving the maximum in component B composition $x_{j,\mathrm{B,max}}$, and $T_{10}$ is the most sensitive tray. Vapor boilup changes of ±5% indicate that $T_{10}$ has a quite symmetric response, as shown in Figure 7b.

We now compare the temperature response of these three possible control-tray locations using a rigorous, nonlinear dynamic simulation of the column.[13] For a given control structure, decentralized PI controllers are tuned automatically. First, the ultimate gain and ultimate period are identified using sequential relay feedback as presented by Shen and Yu.[14] Then, the PI controller settings are obtained following the Tyreus and Luyben[15] tuning rule. Figure 8 shows a ±10% $Z_B/Z_C$ change. What we can observe is that the temperature dynamics give somewhat comparable speeds of response. However, when we use a temperature-control tray below the maximum $x_{i,\mathrm{B,max}}$, we get much more sluggish composition dynamics. Similar behavior is observed for feed flow rate and $Z_A$ changes.

**2.3. Isotherms in Composition Space.** To explain more quantitatively what we observe with the closed-loop simulations, we can look at temperature isotherms in composition space (since we are controlling temperature in the column as a proxy for composition). From vapor−liquid equilibrium (VLE), we have

$$y_i P = x_i P_i^{\mathrm{sat}} \tag{1}$$

where $y_i$ and $x_i$ are the mole fractions in the vapor and

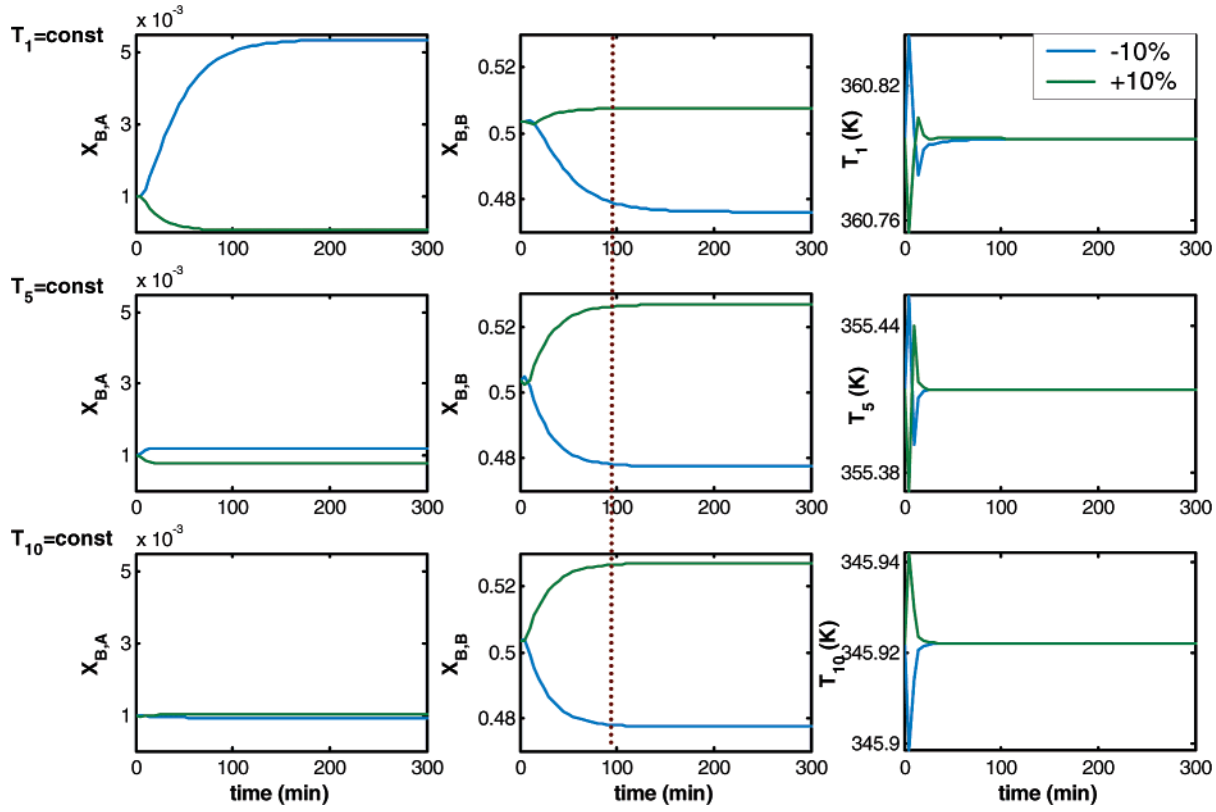


**Figure 8.** Closed-loop responses with different temperature-control trays ($T_1$, $T_5$, and $T_{10}$ control) for ±10% $Z_B/Z_C$ changes.

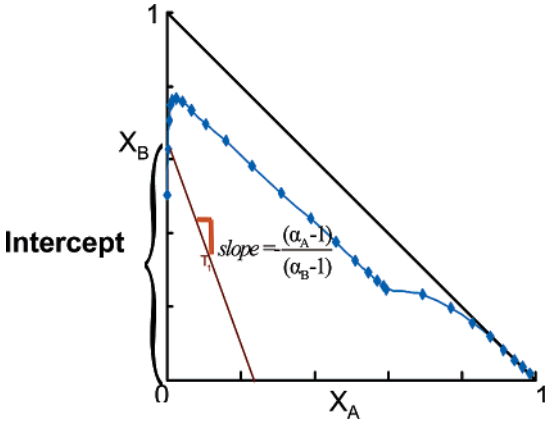


**Figure 9.** Constant temperature line in the composition space.

liquid phases, $P$ is the total pressure, and $P_i^{sat}$ is the vapor pressure of the pure components. We know that the sum of the vapor mole fractions and the total pressure must satisfy

$$\sum y_i = 1 = \Sigma \frac{x_i P_i^{sat}}{P} \tag{2}$$

$$P = \Sigma x_i P_i^{sat} \tag{3}$$

From the Clausius−Clapeyron equation, we can relate the vapor pressure to temperature via a reference temperature and vapor pressure.

$$P_i^{sat} = P_{i,0} \exp\left[-\frac{\Delta H_i}{R}\left(\frac{1}{T} - \frac{1}{T_0}\right)\right] \tag{4}$$

where $\Delta H_i$ is the molar heat of vaporization and $R$ is the gas constant. At low pressure with constant relative volatilities

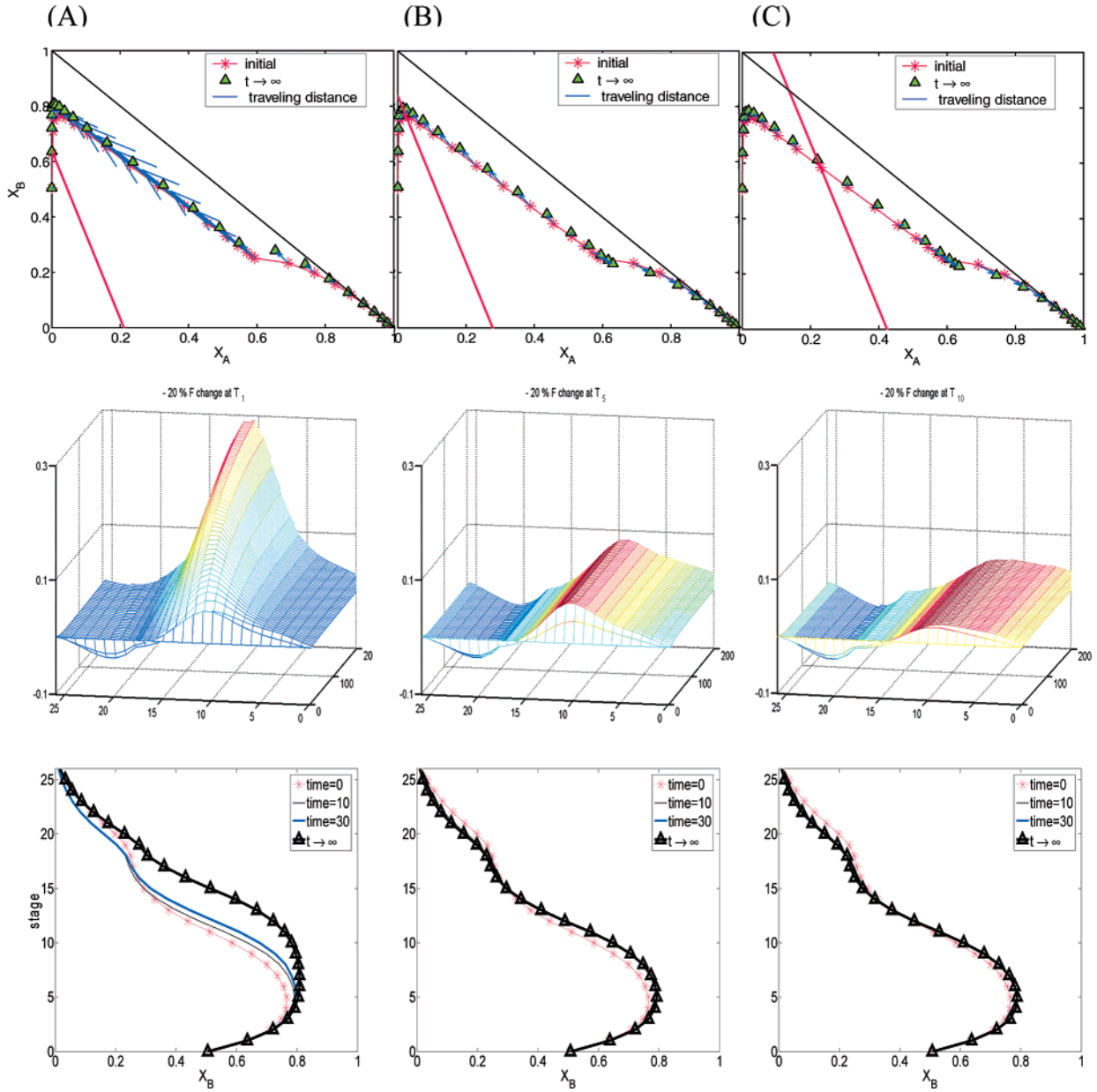


**Figure 10.** Reshaping composition profile for −20% $F$ change with (A) $T_1$ control, (B) $T_5$ control, and (C) $T_{10}$ control for: (top) initial and final composition profiles with traveling distance (shown by arrow), (middle) evolution of composition profile of B, and (bottom) snapshots of composition profile of B as time approaches 0, 10, 30, and ∞.

$$K_i = \frac{P_i^{sat}}{P} = \frac{P_i^{sat}}{\sum x_i P_i^{sat}} = \frac{\alpha_i}{\sum \alpha_i x_i} \quad (5)$$

where $K_i$ is the $K$-value of the $i$th component.

Equal molar overflow assumes $\Delta H_i$ is constant over the temperature range of interest for all components, $\Delta H_i = \Delta H$. We can obtain

$$\frac{1}{T} - \frac{1}{T_0} = \frac{R}{\Delta H} \ln \frac{(\sum x_i \alpha_i)}{(\sum x_i \alpha_i)_0} \quad (6)$$

If we let the heavy component C be the reference component ($x_A = x_B = 0$ and $x_C = 1$ with $\alpha_C = 1$), we get $(\sum x_i \alpha_i)_0 = ((0 \times 4) + (0 \times 2) + (1 \times 1)) = 1$. After some rearrangement, we have

$$\frac{1}{T} - \frac{1}{T_C^{sat}} = \frac{R}{\Delta H} \ln(\sum x_i \alpha_i) = \frac{R}{\Delta H} \ln(\alpha_A x_A + \alpha_B x_B + \alpha_C x_C) \quad (7)$$

where $T_C^{sat}$ is the boiling-point temperature of component C at the given pressure. Finally, we get

$$\exp\left[\frac{\Delta H}{R}\left(\frac{1}{T} - \frac{1}{T_C^{sat}}\right)\right] = (\alpha_A - 1)x_A + (\alpha_B - 1)x_B + 1$$

and

$$x_B = -\frac{(\alpha_A - 1)}{(\alpha_B - 1)} x_A + \frac{1}{(\alpha_B - 1)}\left\{\exp\left[\frac{\Delta H^{vap}}{R}\left(\frac{1}{T} - \frac{1}{T_C^{sat}}\right)\right] - 1\right\} \quad (8)$$

This is an equation for a straight line in $x_A - x_B$ space with a slope and intercept for temperature isotherm lines. The slope is $-(\alpha_A - 1)/(\alpha_B - 1)$ and the intercept can be expressed as $(1/(\alpha_B - 1))\{\exp[(\Delta H/R)((1/T) - (1/T_C^{sat}))] - 1\}$. This is shown in Figure 9. So when we use a temperature for control with a constant setpoint, the direction of movement is along this isotherm line.

**2.4. Analysis.** Figure 10 shows what happens to the column composition profile for a 20% decrease in feed flow with the three different constant temperature-control trays. With constant $T_1$ (the temperature has to lie on the temperature isotherm), the column composition profile has to change much more than with constant $T_{10}$, as shown in the first row of Figure 10. Despite the fact that the final column composition profiles almost coincide with the initial one for all three cases, the tray composition is very different from the nominal one when $T_1$ is kept constant. The 3-D plots in the second row of Figure 10 reveal that the column takes a longer time to settle if the tray composition travels a significant distance in the composition space. The snapshots of the composition profile of component B at times (in min) approaching 0, 10, 30, and ∞ show very different speeds of response for $T_1$, $T_5$, and $T_{10}$ control.

The following observations can be made immediately. First, under a load change, the entire column composition profile covered by the column does not change much, at least visually. Second, the internal (tray) compositions may be very different using different temperature-control trays. Third, the distance each tray composition travels (in the composition space) is associated with the speed of response. Similar behavior is also observed for $Z_A$ and $Z_B/Z_C$ disturbances.

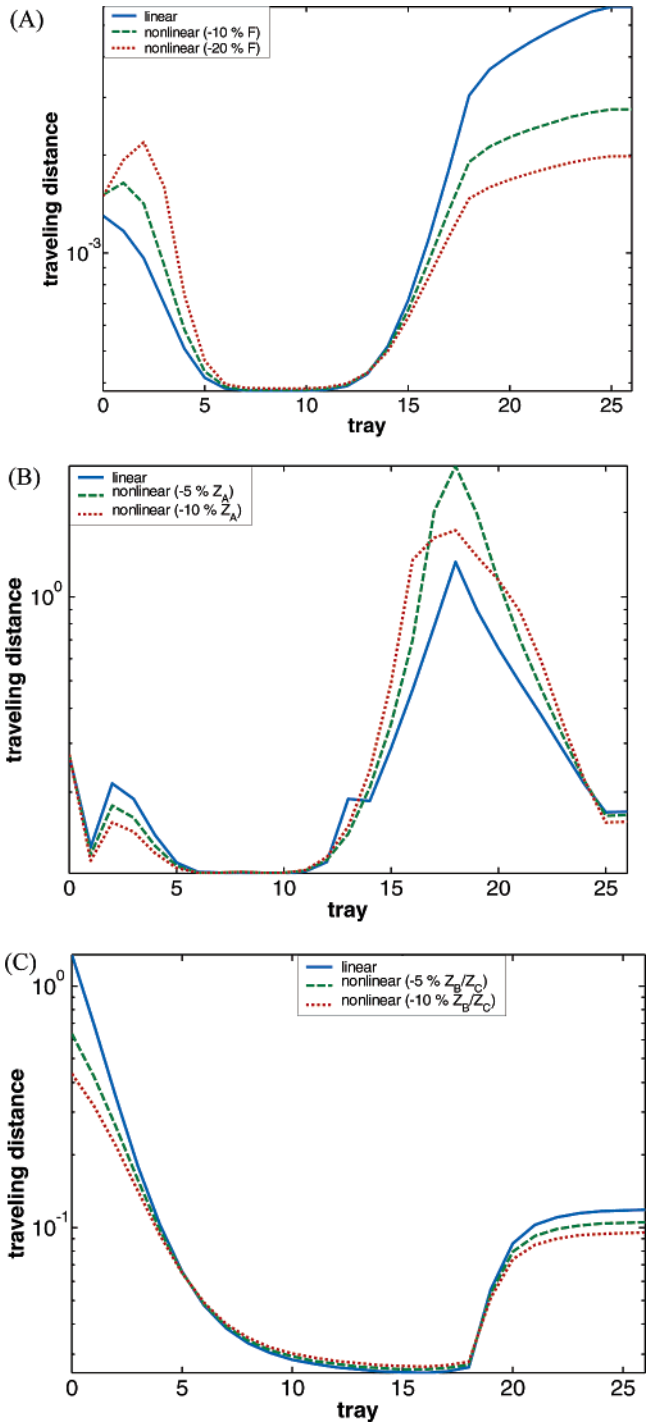


**Figure 11.** Traveling distance from linear analysis and nonlinear simulation for: (A) $F$, (B) $Z_A$, and (C) $Z_B/Z_C$ changes.

We can also calculate a quantitative measure, called the traveling distance, to compare how much the composition profile needs to change with tray temperatures held constant. This nomenclature is inspired by the wave propagation theory of Hwang[16] and Kienle,[17] where the composition profile is treated as a wave traveling up and down the column. Here, we are interested in the distance the wave travels. We derive the traveling distance from the linearized open-loop transfer function

$$\begin{bmatrix} x_{1,1} \\ \vdots \\ x_{\mathrm{NT},1} \\ x_{1,2} \\ \vdots \\ x_{\mathrm{NT},2} \\ T_1 \\ \vdots \\ T_{\mathrm{NT}} \end{bmatrix} = \begin{bmatrix} G_{1,1} \\ \vdots \\ G_{\mathrm{NT},1} \\ G_{1,2} \\ \vdots \\ G_{\mathrm{NT},2} \\ G_{T_1} \\ \vdots \\ G_{T\mathrm{NT}} \end{bmatrix} [u] + \begin{bmatrix} G_{\mathrm{L}1,1} \\ \vdots \\ G_{\mathrm{LNT},1} \\ G_{\mathrm{L}1,2} \\ \vdots \\ G_{\mathrm{LNT},2} \\ G_{\mathrm{L}T_1} \\ \vdots \\ G_{\mathrm{L}T\mathrm{NT}} \end{bmatrix} [d] \tag{9}$$

where $x_{j,i}$ is the molar fraction of the component $i$ of the $j$th tray, $T_j$ is the temperature of the $j$th tray, $G_{j,i}$ is the process transfer function of the component $i$ of the $j$th tray, $G_{T_j}$ is the process transfer function of the $j$th temperature-control tray, $G_{\mathrm{L}j,i}$ is the load transfer function of the component $i$ of the $j$th tray, $G_{\mathrm{L}T_j}$ is the load transfer function of the $j$th temperature-control tray, $u$ is the manipulated variable, and $d$ is the load variable.

Under the assumption of perfect temperature control,

$$T_j = G_{T_j} u + G_{\mathrm{L}T_j} d = 0 \tag{10}$$

we can get the value of the manipulated variable under closed-loop control.

$$u^{\mathrm{CL}} = -\frac{G_{\mathrm{L}T_j}}{G_{T_j}} d \tag{11}$$

This leads to

$$\begin{aligned} x_{j,i} &= G_{j,i} u^{\mathrm{CL}} + G_{\mathrm{L}j,i} d \\ &= G_{j,i}\left(-\frac{G_{\mathrm{L}T_j}}{G_{T_j}} d\right) + G_{\mathrm{L}j,i} d \\ &= \left(-\frac{G_{\mathrm{L}T_j} G_{j,i}}{G_{T_j}} + G_{\mathrm{L}j,i}\right) d \\ &= G^*_{\mathrm{L}j,i} d \end{aligned} \tag{12}$$

Then,

$$\begin{bmatrix} x_{1,1} \\ \vdots \\ x_{\mathrm{NT},1} \\ x_{1,2} \\ \vdots \\ x_{\mathrm{NT},2} \end{bmatrix} = \begin{bmatrix} G_{\mathrm{L}1,1} - G_{1,1}\left(\dfrac{G_{\mathrm{L}T_j}}{G_{T_j}}\right) \\ \vdots \\ G_{\mathrm{LNT},1} - G_{\mathrm{NT},1}\left(\dfrac{G_{\mathrm{L}T_j}}{G_{T_j}}\right) \\ G_{\mathrm{L}1,2} - G_{1,2}\left(\dfrac{G_{\mathrm{L}T_j}}{G_{T_j}}\right) \\ \vdots \\ G_{\mathrm{LNT},2} - G_{\mathrm{NT},2}\left(\dfrac{G_{\mathrm{L}T_j}}{G_{T_j}}\right) \end{bmatrix} [d] = \begin{bmatrix} G^*_{\mathrm{L}1,1} \\ \vdots \\ G^*_{\mathrm{LNT},1} \\ G^*_{\mathrm{L}1,2} \\ \vdots \\ G^*_{\mathrm{LNT},2} \end{bmatrix} [d] \tag{13}$$

We define the absolute traveling distance as

$$\Delta x_j = \left(\sum_{i=1}^{\mathrm{NC}-1} {x_{j,i}}^2\right)^{1/2} = \left({x_{j,1}}^2 + {x_{j,2}}^2\right)^{1/2} \tag{14}$$

The normalized traveling distance is

$$\frac{\|\Delta x\|_2}{\|d\|_2}/\mathrm{NT} \left\| \begin{bmatrix} [(G^*_{\mathrm{L}1,1})^2 + (G^*_{\mathrm{L}1,2})^2]^{1/2} \\ \vdots \\ [(G^*_{\mathrm{LNT},1})^2 + (G^*_{\mathrm{LNT},2})^2]^{1/2} \end{bmatrix} \right\|_2 /\mathrm{NT} \tag{15}$$

Figure 11A shows a plot of the traveling distance for a change in $F$. The solid line is computed from the linear analysis (eq 15), the dashed line is obtained from the nonlinear column simulation for a $-10\%$ $F$ change, and the dotted line is also the result of the nonlinear simulation with a $-20\%$ feed flow change. Qualitatively similar shapes can be seen in Figure 11A where $T_1$ control gives a large traveling distance as compared to $T_5$ and $T_{10}$ control. Note that here we intend to control bottoms composition with vapor boilup as the manipulated variable, so the trays of interest should lie below the feed tray ($T_1$–$T_{18}$). Figure 11B shows the traveling distance for a $Z_A$ change, and Figure 11C shows the traveling distance for a $Z_B/Z_C$ change. The time-domain behavior in Figure 10 can be explained by the quantitative measure, and the results indicate that, the smaller the traveling distance, the better it is for stabilizing the composition profile in the column. Compared to single-temperature control, the dual-end control provides a much more critical test for the appropriateness of the temperature-control trays, and this is understandable because two temperatures are restricted on the isotherms (e.g., Figure 14).

**2.5. Dual-End Control.** If we now consider dual-end control, where we use two column temperatures to control distillate and bottoms purities, we can look at how we select the two temperatures. Using the non-square relative gain (NRG),[4] we would choose the top temperature-control tray on theoretical stage 19. We will use two choices for the bottoms temperature-control trays on stage 1 or 9. The NRG is used for the measurement selection.

$$\Lambda^{\mathrm{N}} = K \otimes (K^{+})^{\mathrm{T}} \tag{16}$$

Here, $\Lambda^{\mathrm{N}}$ stands for the NRG, $\otimes$ denotes element-by-element multiplication, the superscripts T and + correspond to transpose and pseudo-inverse, respectively. Figure 12 shows the row sum of the NRG for the dual-end temperature-control problem. The analysis shows that $T_9$ and $T_{19}$ are the recommended temperature-control trays. Again, the concept of traveling distance can be used to explore the potential problem in dual-temperature control.

The traveling distance for dual-end control can be derived from the open-loop transfer function. Consider the following process transfer function matrices.

$$\begin{bmatrix} x_{1,1} \\ \vdots \\ x_{\mathrm{NT},1} \\ x_{1,2} \\ \vdots \\ x_{\mathrm{NT},2} \\ T_1 \\ \vdots \\ T_{\mathrm{NT}} \end{bmatrix} = \begin{bmatrix} G^{(1)}_{1,1} & G^{(2)}_{1,1} \\ \vdots & \vdots \\ G^{(1)}_{\mathrm{NT},1} & G^{(2)}_{\mathrm{NT},1} \\ G^{(1)}_{1,2} & G^{(2)}_{1,2} \\ \vdots & \vdots \\ G^{(1)}_{\mathrm{NT},2} & G^{(2)}_{\mathrm{NT},2} \\ G^{(1)}_{T_1} & G^{(2)}_{T_1} \\ \vdots & \vdots \\ G^{(1)}_{T\mathrm{NT}} & G^{(2)}_{T\mathrm{NT}} \end{bmatrix} \begin{bmatrix} u_1 \\ u_2 \end{bmatrix} + \begin{bmatrix} G_{\mathrm{L}1,1} \\ \vdots \\ G_{\mathrm{LNT},1} \\ G_{\mathrm{L}1,2} \\ \vdots \\ G_{\mathrm{LNT},2} \\ G_{\mathrm{LT}1} \\ \vdots \\ G_{\mathrm{L}T\mathrm{NT}} \end{bmatrix} [d] \tag{17}$$

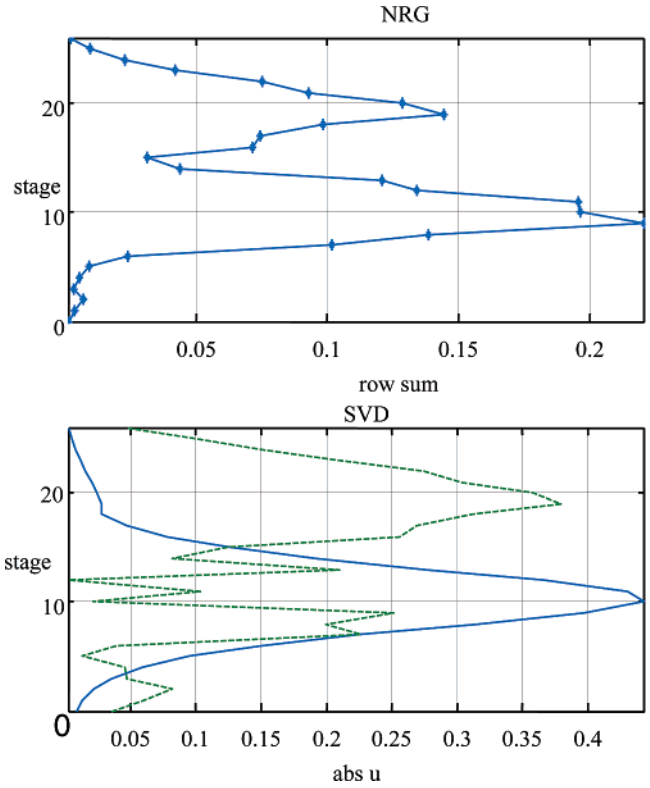


**Figure 12.** Row sum of NRG for dual-end temperature control using reflux flow and vapor boilup as manipulated variables.

where $x_{j,i}$ is the molar fraction of the component $i$ of the $j$th tray, $T_j$ is the temperature of the $j$th tray, $G_{j,i}^{(k)}$ is the process transfer function of the component $i$ of the $j$th tray under the $k$th manipulated variables, $G_{T_j}^{(k)}$ is the process transfer function of the $j$th temperature-control tray under the $k$th manipulated variable, $G_{Lj,i}$ is the load transfer function of the component $i$ of the $j$th tray, and $G_{LT_j}$ is the load transfer function of the $j$th temperature-control tray.

If $T_l$ and $T_m$ are under perfect control,

$$T_l = G_{T_l}^{(1)}u_1 + G_{T_l}^{(2)}u_2 + G_{LT_l}d = 0$$
$$T_m = G_{T_m}^{(1)}u_1 + G_{T_m}^{(2)}u_2 + G_{LT_m}d = 0 \qquad (18)$$

we can get

$$u_1^{CL} = \frac{(-G_{T_m}^{(2)}G_{LT_l} + G_{LT_m}G_{T_l,2})}{(G_{T_l}^{(1)}G_{T_m}^{(2)} - G_{T_l}^{(2)}G_{T_m}^{(1)})}d$$
$$u_2^{CL} = \frac{(-G_{T_l}^{(1)}G_{LT_m} + G_{L,1}G_{T_m}^{(1)})}{(G_{T_l}^{(1)}G_{T_m}^{(2)} - G_{T_l}^{(2)}G_{T_m}^{(1)})}d \qquad (19)$$

Substituting $u_1^{CL}$ and $u_2^{CL}$ into eq 18 and rearranging, we have

$$\begin{bmatrix} x_{1,1} \\ \vdots \\ x_{NT,1} \\ x_{1,2} \\ \vdots \\ x_{NT,2} \end{bmatrix} = \begin{bmatrix} G_{L1,1}^* \\ \vdots \\ G_{LNT,1}^* \\ G_{L1,2}^* \\ \vdots \\ G_{LNT,2}^* \end{bmatrix} [d]$$

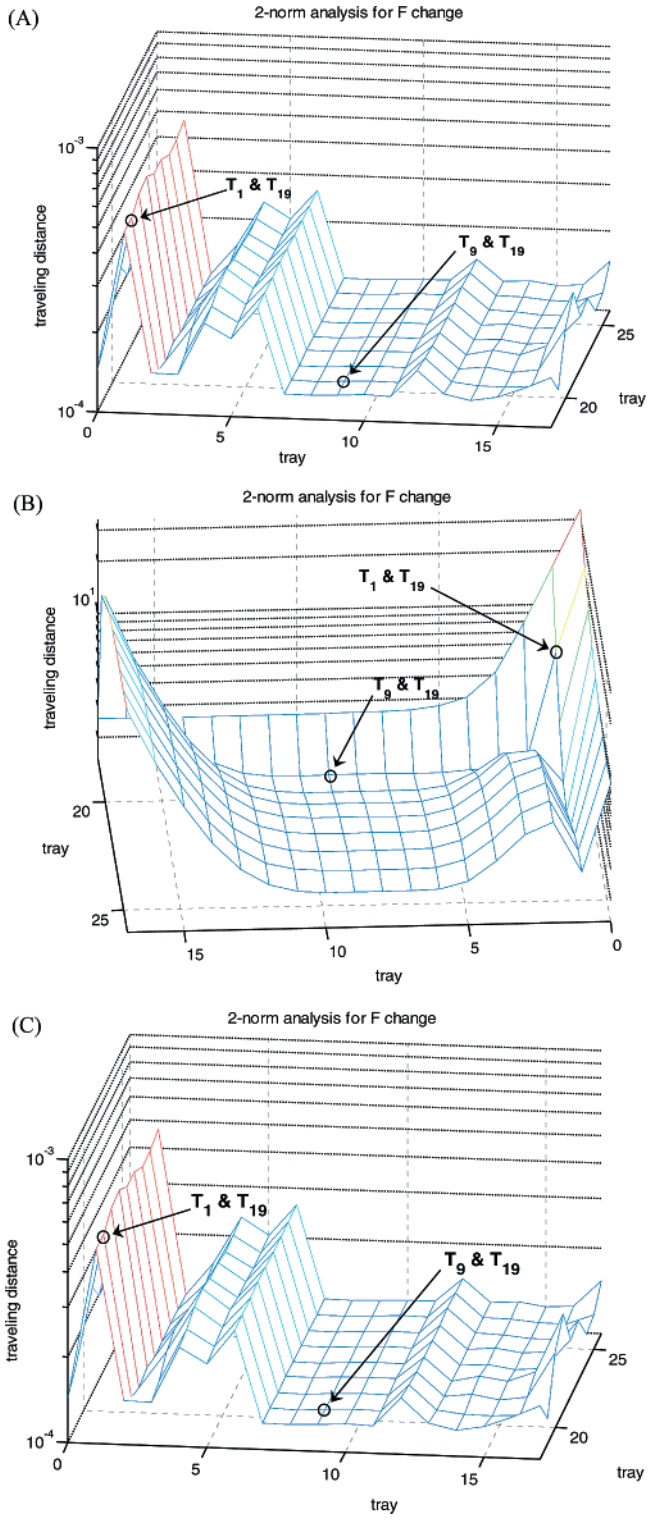


**Figure 13.** Traveling distance for dual-end control with: (A) $F$, (B) $Z_A$, and (C) $Z_B/Z_C$ changes.

The traveling distance for dual-end control becomes

$$\frac{||\Delta x||_2}{||d||_2}/\mathrm{NT} = \left\| \begin{bmatrix} [(G_{L1,1}^*)^2 + (G_{L1,2}^*)^2]^{1/2} \\ \vdots \\ [(G_{LNT,1}^*)^2 + (G_{LNT,2}^*)^2]^{1/2} \end{bmatrix} \right\|_2 /\mathrm{NT} \quad (20)$$

Figure 13 shows the traveling distance for dual-end control for $F$, $Z_A$, and $Z_B/Z_C$ changes. Here, we limit ourselves to the pairing of the lower part of the temperatures (below feed tray) with vapor boilup and the

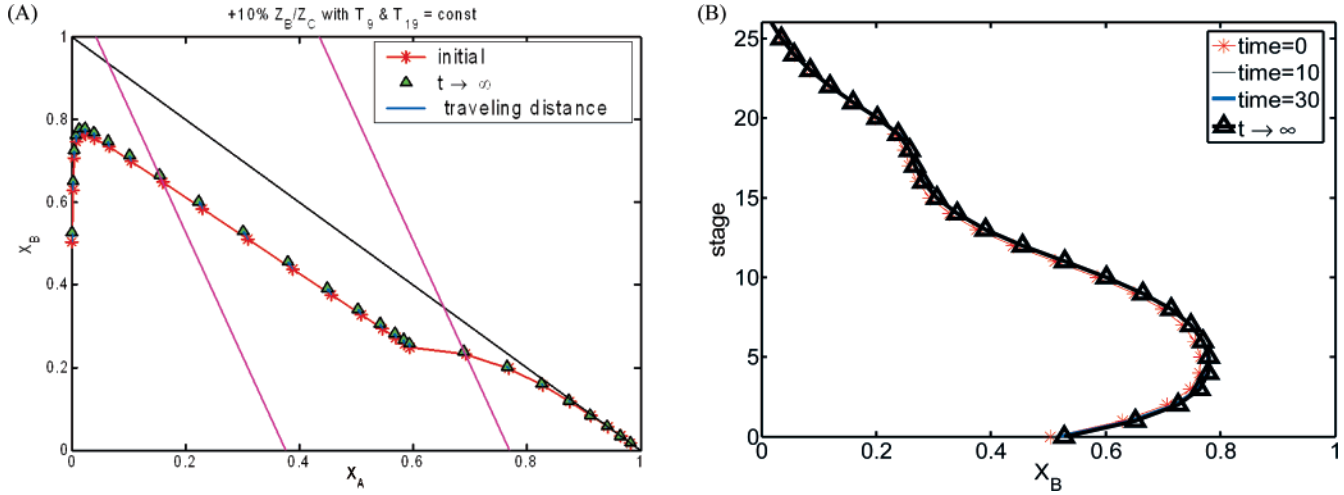


**Figure 14.** Reshaping composition profile with $T_9 - T_{19}$ control for +10% $Z_B/Z_C$ change for: (A) initial & final composition profiles with traveling distance (shown by arrow) and (B) snapshots of composition profile of B as time approaches 0, 10, 30, and ∞.

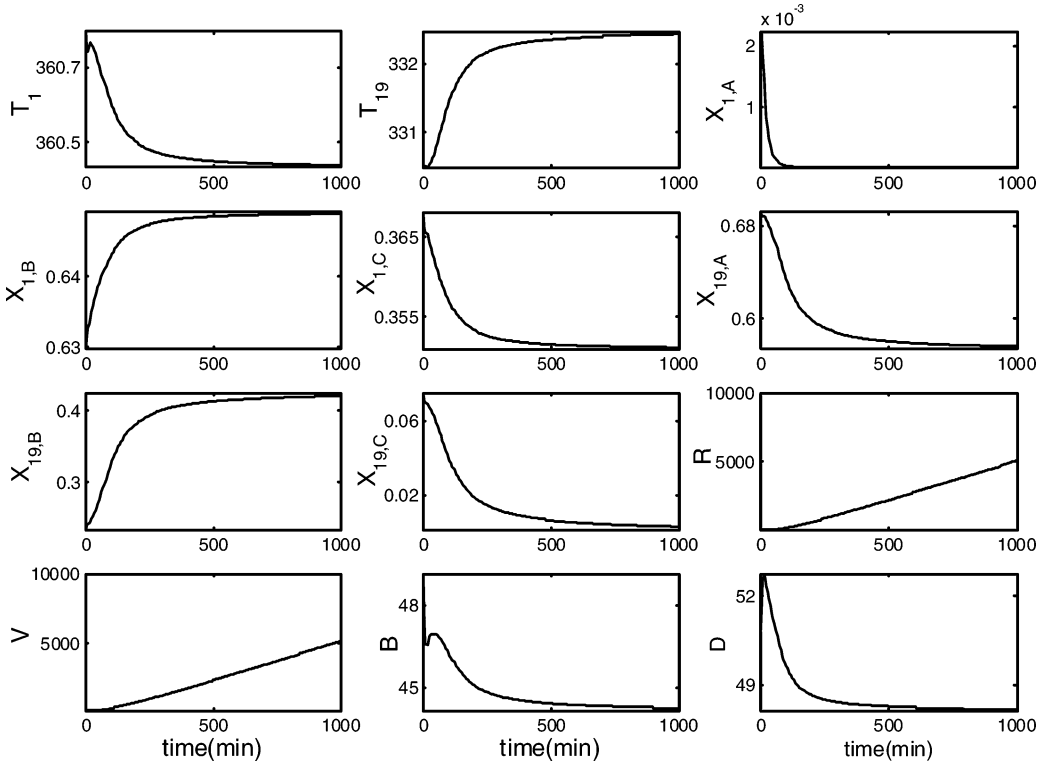


**Figure 15.** Internally unstable closed-loop responses with $T_1 - T_{19}$ control for +10% $Z_B/Z_C$ change.

upper part of the temperatures (above feed tray) with reflux flow rate. The quantitative measure clearly shows that, indeed, $T_9$ and $T_{19}$ are better choices as compared to, for example, $T_1$ and $T_{19}$. Rigorous nonlinear simulation indicates that dual-end control by keeping $T_9$ and $T_{19}$ constant gives good composition dynamics, as shown in Figure 14, where the profile of component B reaches steady-state in 10 min for a 10% increase in $Z_B/Z_C$. On the other hand, the $T_1$ and $T_{19}$ dual-end control fails to stabilize the column for the same disturbance, as can be seen in Figure 15. The reason is that the increase in the intermediate boiler (component B) shifts the profile upward in the composition space (e.g., Figure 14A). It is not possible to hold tray 1 temperature at setpoint (not letting excess B out of the system) while maintaining tray 19 temperature at setpoint. If these two temperatures ($T_1$ and $T_{19}$) are used, one way to avoid instability is to use proportional-only temperature control or to change the value of the controller setpoint.

**2.6. Interaction between "Process" and "Control" Direction.** Why does $T_1$ control (single- or dual-end) result in a large traveling distance and, consequently, sluggish response? For temperature control, the "control direction" is fixed to the temperature isotherm, as shown in Figure 10. Regardless of the types of disturbances, that implies the composition on tray 1 has to lie on that isotherm. The process, on the other hand, generally moves along the tangent of the composition profile (distillation line), the "process" direction. Let us take the −20% feed flow change in Figure 10 as an example. The disturbance pushes the tray 1 composition further down toward the C corner along the B−C edge (the process direction). The $T_1$ control, however, tries to move the tray 1 composition away from the B−C edge

along the $T_1$ isotherm (the control direction), but not by much (because little A remains in the lower part of the column). Because a smaller amount of heavies than necessary is allowed to leave the column base, we have a build-up of B and C in the column that has to percolate through to the composition redistribution, as can be seen in Figure 10. Certainly, the feed flow is altered, so we need to change the process direction. Relatively speaking, the conflict between the process and control directions is less severe for $T_{10}$ control because of better maneuverability for tray 10 composition. The interaction between the process and control directions is not limited to temperature control only; it can become even more severe for direct composition control.

## 3. Extension to Composition Control

**3.1. Control Direction for Composition Control.** Composition control in multicomponent systems differs from the binary system, since we have the freedom to select the controlled variable (e.g., purity, impurity, ratio of key components, etc.). This affects the control direction, as shown in Figure 16. When composition A is under control ($x_{j\mathrm{A}}$ = constant), the control direction is parallel to the B−C edge. Similarly, we can move the control direction perpendicular to the B−C edge by controlling $x_{j\mathrm{B}}$ or we can make it parallel to the A−B edge by keeping $x_{j\mathrm{C}}$ constant.

**3.2. Single-End Control.** Similar to the case of temperature control, the traveling distance for single-end composition control can be derived analytically, provided we have the steady-state gain matrices.

$$\begin{bmatrix} x_{1,1} \\ \vdots \\ x_{\mathrm{NT},1} \\ x_{1,2} \\ \vdots \\ x_{\mathrm{NT},2} \end{bmatrix} = \begin{bmatrix} G_{1,1} \\ \vdots \\ G_{\mathrm{NT},1} \\ G_{1,2} \\ \vdots \\ G_{\mathrm{NT},2} \end{bmatrix} [u] + \begin{bmatrix} G_{\mathrm{L}1,1} \\ \vdots \\ G_{\mathrm{LNT},1} \\ G_{\mathrm{L}1,2} \\ \vdots \\ G_{\mathrm{LNT},2} \end{bmatrix} [d] \tag{21}$$

Assume $x_{j,i}$ is under perfect composition control,

$$x_{j,i} = G_{j,i}u + G_{\mathrm{L}j,i}d = 0 \tag{22}$$

We can get

$$u^{\mathrm{CL}} = -\frac{G_{\mathrm{L}j,i}}{G_{j,i}}d \tag{23}$$

When we substitute $u^{\mathrm{CL}}$ into eq 22 and rearrange, we have

$$\begin{bmatrix} x_{1,1} \\ \vdots \\ x_{\mathrm{NT},1} \\ x_{1,2} \\ \vdots \\ x_{\mathrm{NT},2} \end{bmatrix} = \begin{bmatrix} G_{\mathrm{L}1,1} - G_{1,1}\left(\dfrac{G_{\mathrm{L}j,i}}{G_{j,i}}\right) \\ \vdots \\ G_{\mathrm{LNT},1} - G_{\mathrm{NT},1}\left(\dfrac{G_{\mathrm{L}j,i}}{G_{j,i}}\right) \\ G_{\mathrm{L}1,2} - G_{1,2}\left(\dfrac{G_{\mathrm{L}j,i}}{G_{j,i}}\right) \\ \vdots \\ G_{\mathrm{LNT},2} - G_{\mathrm{NT},2}\left(\dfrac{G_{\mathrm{L}j,i}}{G_{j,i}}\right) \end{bmatrix} [d] = \begin{bmatrix} G^*_{\mathrm{L}1,1} \\ \vdots \\ G^*_{\mathrm{LNT},1} \\ G^*_{\mathrm{L}1,2} \\ \vdots \\ G^*_{\mathrm{LNT},2} \end{bmatrix} [d] \tag{24}$$

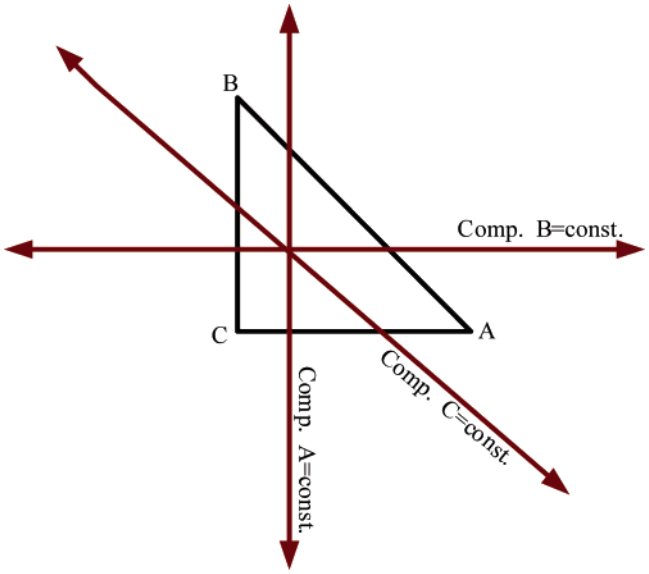


**Figure 16.** Control directions with $x_{j,\mathrm{A}}$, $x_{j,\mathrm{B}}$, and $x_{j,\mathrm{C}}$ control in the composition space.

The traveling distance is

$$\frac{||\Delta x||_2}{||d||_2}/\mathrm{NT} = \left\| \begin{matrix} \{(G^*_{\mathrm{L}1,1})^2 + (G^*_{\mathrm{L}1,2})^2\}^{1/2} \\ \vdots \\ \{(G^*_{\mathrm{LNT},1})^2 + (G^*_{\mathrm{LNT},2})^2\}^{1/2} \end{matrix} \right\|_2 /\mathrm{NT} \tag{25}$$

Let us use the bottoms composition control to illustrate the effect of the control direction (by choosing different components to control) on the closed-loop performance. First, the traveling distance for controlling $x_{\mathrm{B,A}}$, $x_{\mathrm{B,B}}$, and $x_{\mathrm{B,C}}$ are computed according to eq 26. Figure 17 reveals that, as expected, $x_{\mathrm{B,A}}$ control gives the smallest traveling distance for all three disturbance, because the control direction coincides with the process direction. Also $x_{\mathrm{B,B}}$ control will give the worst performance because of its large traveling distance, where $x_{\mathrm{B,C}}$ control lies somewhere between the two. The traveling distances for composition control are put in the same graph with that of temperature control. Rigorous nonlinear simulations show that the conflict between the process and control directions using $x_{\mathrm{B,B}}$ and $x_{\mathrm{B,C}}$ gives more sluggish responses. This can be seen in the snapshots of the $x_{j,\mathrm{B}}$ control composition profiles in Figure 18. Much larger traveling distances are observed for $x_{\mathrm{B,B}}$ and $x_{\mathrm{B,C}}$ control. On the other hand, $x_{\mathrm{B,A}}$ control leads to faster composition dynamics as a result of a much smaller traveling distance.

**3.3. Dual-Composition Control.** The traveling distance for dual-end composition control can be derived from the open-loop transfer function in a similar way as above.

$$\begin{bmatrix} x_{1,1} \\ \vdots \\ x_{\mathrm{NT},1} \\ x_{1,2} \\ \vdots \\ x_{\mathrm{NT},2} \end{bmatrix} = \begin{bmatrix} G^{(1)}_{1,1} & G^{(2)}_{1,1} \\ \vdots & \vdots \\ G^{(1)}_{\mathrm{NT},1} & G^{(2)}_{\mathrm{NT},1} \\ G^{(1)}_{1,2} & G^{(2)}_{1,2} \\ \vdots & \vdots \\ G^{(1)}_{\mathrm{NT},2} & G^{(2)}_{\mathrm{NT},2} \end{bmatrix} \begin{bmatrix} u_1 \\ u_2 \end{bmatrix} + \begin{bmatrix} G_{\mathrm{L}1,1} \\ \vdots \\ G_{\mathrm{LNT},1} \\ G_{\mathrm{L}1,2} \\ \vdots \\ G_{\mathrm{LNT},2} \end{bmatrix} [d] \tag{26}$$

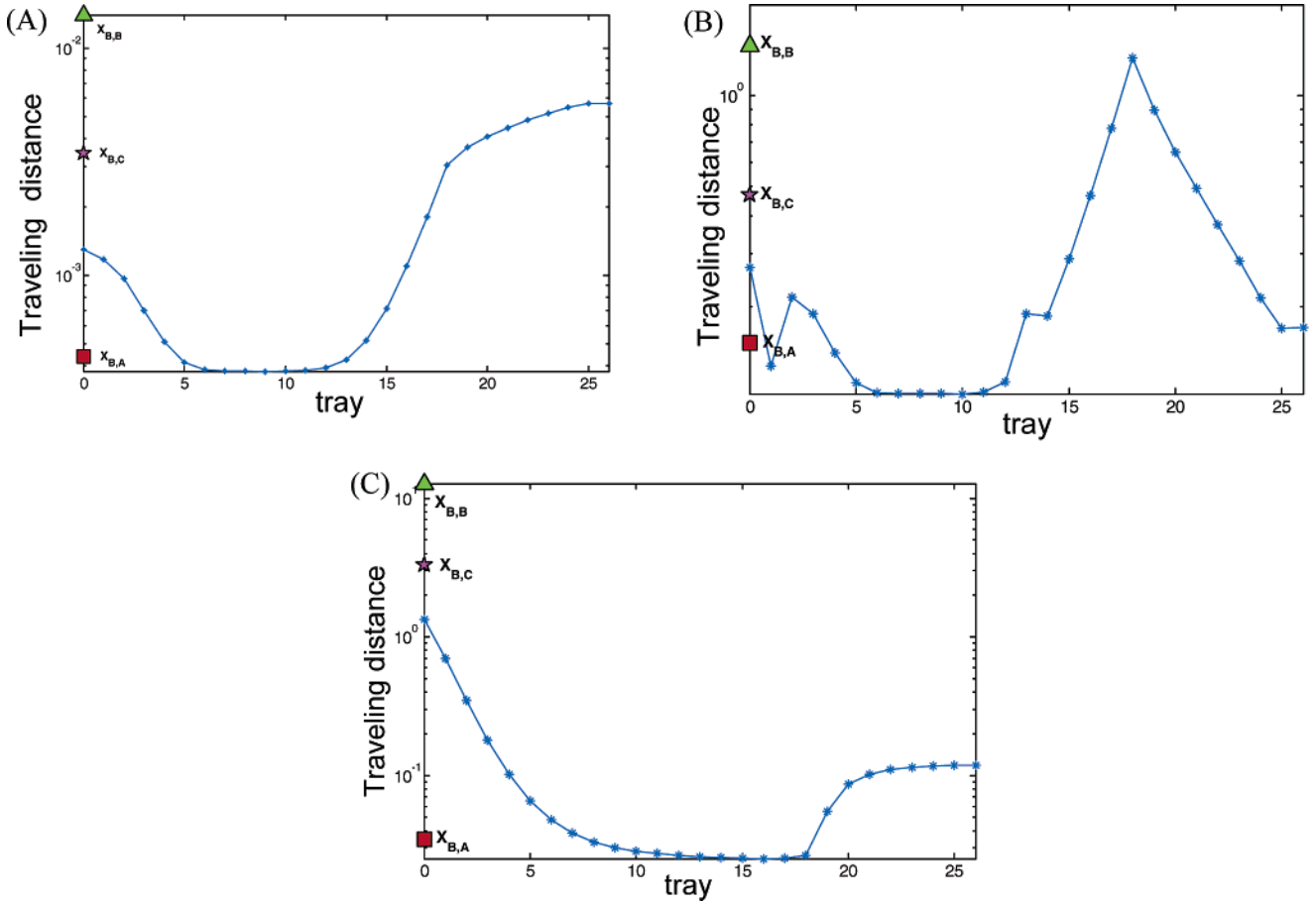


**Figure 17.** Traveling distance for different composition control ($x_{B,A}$, $x_{B,B}$, and $x_{B,C}$) as compared to temperature control for: (A) $F$, (B) $Z_A$, and (C) $Z_B/Z_C$ disturbances.

Under perfect composition control by keeping the $p$th component of the $l$th tray and the $q$th component of the $m$th tray constant, we have

$$x_{l,p} = G^{(1)}_{l,p}u_1 + G^{(2)}_{l,p}u_2 + G_{Ll,p}d = 0$$

$$x_{m,q} = G^{(1)}_{m,q}u_1 + G^{(2)}_{m,q}u_2 + G_{Lm,q}d = 0 \qquad (27)$$

Then

$$u_1^{CL} = \frac{(-G^{(2)}_{m,q}G_{Ll,p} + G_{Lm,q}G^{(2)}_{l,p})}{(G^{(1)}_{l,p}G^{(2)}_{l,p} - G^{(1)}_{m,q}G^{(2)}_{m,q})}d;$$

$$u_2^{CL} = \frac{(-G^{(1)}_{l,p}G_{Lm,q} + G_{Ll,p}G^{(1)}_{m,q})}{(G^{(1)}_{l,p}G^{(2)}_{l,p} - G^{(1)}_{m,q}G^{(2)}_{m,q})}d \qquad (28)$$

Substitute into

$$\begin{bmatrix} x_{1,1} \\ \vdots \\ x_{NT,1} \\ x_{1,2} \\ \vdots \\ x_{NT,2} \end{bmatrix} = \begin{bmatrix} G^*_{L1,1} \\ \vdots \\ G^*_{LNT,1} \\ G^*_{L1,2} \\ \vdots \\ G^*_{LNT,2} \end{bmatrix} [d] \qquad (29)$$

The traveling distance is

$$\frac{||\Delta x||_2}{||d||_2}/NT = \left\| \begin{bmatrix} [(G^*_{L1,1})^2 + (G^*_{L1,2})^2]^{1/2} \\ \vdots \\ [(G^*_{LNT,1})^2 + (G^*_{LNT,2})^2]^{1/2} \end{bmatrix} \right\|_2 /NT \qquad (30)$$

If $x_{B,A}$ control resolves the conflict between the process and control directions at the bottom, we should expect control of composition C, $x_{D,C}$ at the column top, to have similar behavior, which can be seen in Figure 16 where the control direction moves along the A−B edge as the upper section of the composition profile does. However, unlike dual-end temperature control, dual-composition control is able to reestablish the composition profile if one of the controlled compositions is correctly selected. This is because the component material balance constraint has to be met. For example, if $x_{B,A}$ control is used for the bottoms loop, the traveling distance is of the same order of magnitude regardless of which composition is selected to control on the top loop ($x_{D,A}$, $x_{D,B}$, or $x_{D,C}$), as shown in Figure 19 for all three disturbances. The initial and final composition profiles for $x_{B,A} - x_{D,C}$ control and $x_{B,A} - x_{D,B}$ control in Figure 20 confirm that the traveling distances are almost the same for both cases. However, the snapshots of the profiles of B in the second row of Figure 20 indicate that $x_{B,A} - x_{D,B}$ control goes through a much larger deviation as compared to the intuitively correct $x_{B,A} - x_{D,C}$ control. Actually, the initial and final composition profiles almost coincide with each other for these two cases.

The time domain simulations for ±20% feed flow rate changes in Figure 21 clearly indicate drastically differ-

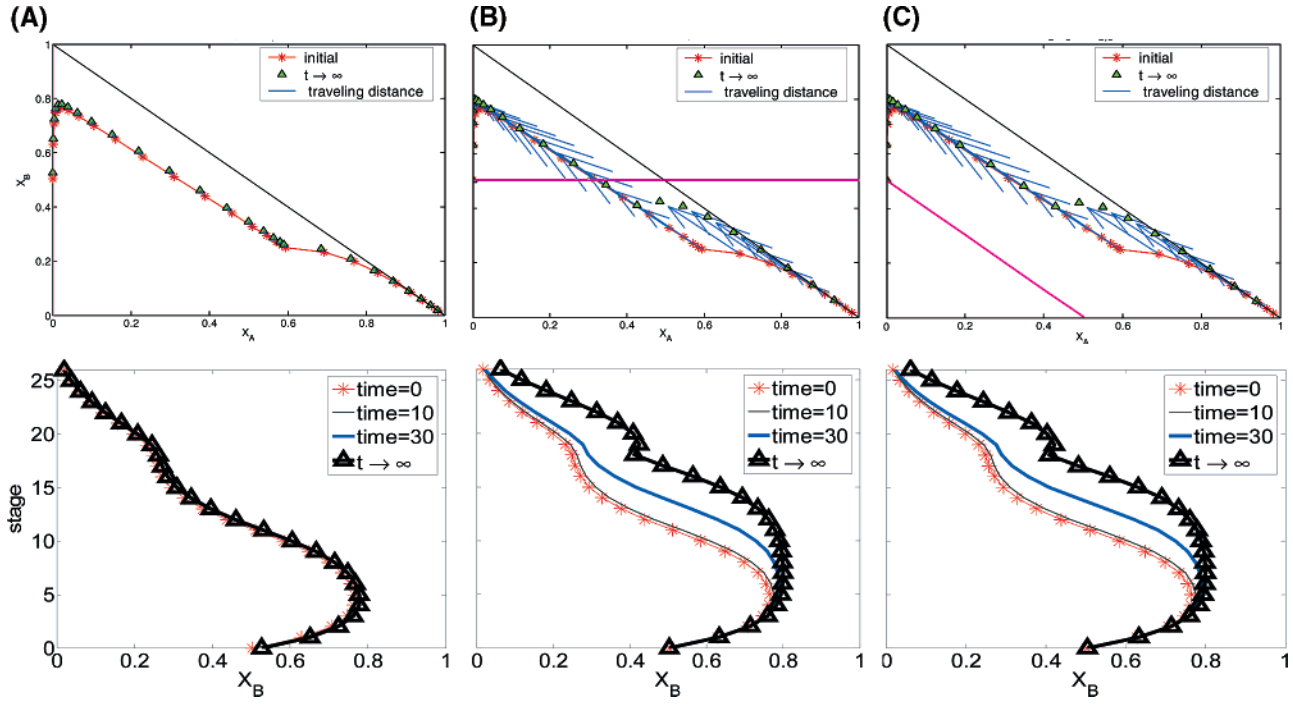


**Figure 18.** Reshaping composition profile for −10% $Z_B/Z_C$ change with (A) $x_{B,A}$ control, (B) $x_{B,B}$ control, and (C) $x_{B,C}$ control: (top) initial and final composition profiles with traveling distance (shown by arrow) and (bottom) snapshots of composition profile of B as time approaches 0, 10, 30, and ∞.

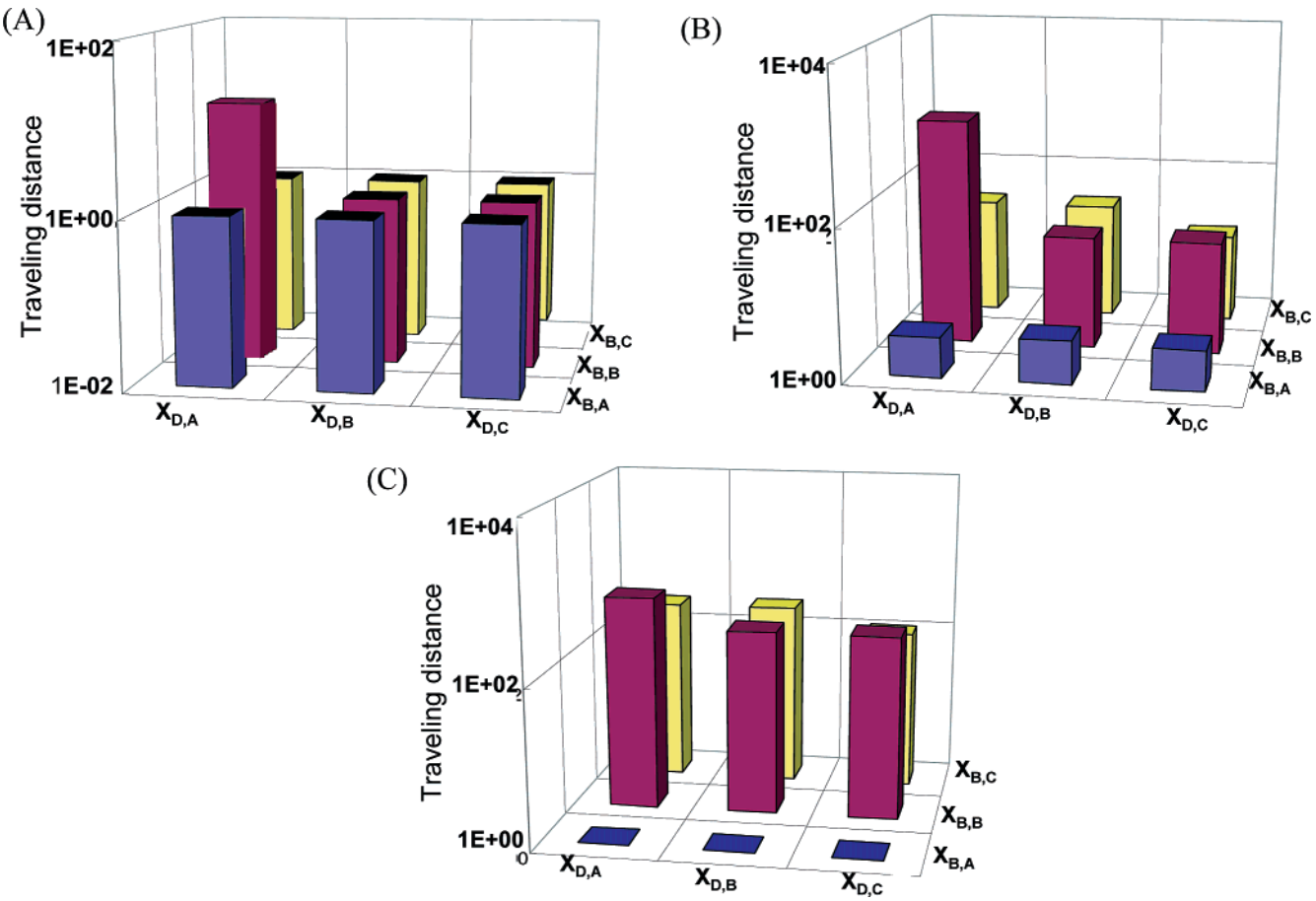


**Figure 19.** Traveling distance under dual-composition control with different composition combinations for: (A) $F$, (B) $Z_A$, and (C) $Z_B/Z_C$ changes.

ent speeds of response for these two control structures, despite having almost the same final steady-state. The dual-composition control example points out the possible limitation of the traveling distance analysis. Because the measure is computed from steady-state gain matrices, it only serves as a sufficient condition for control

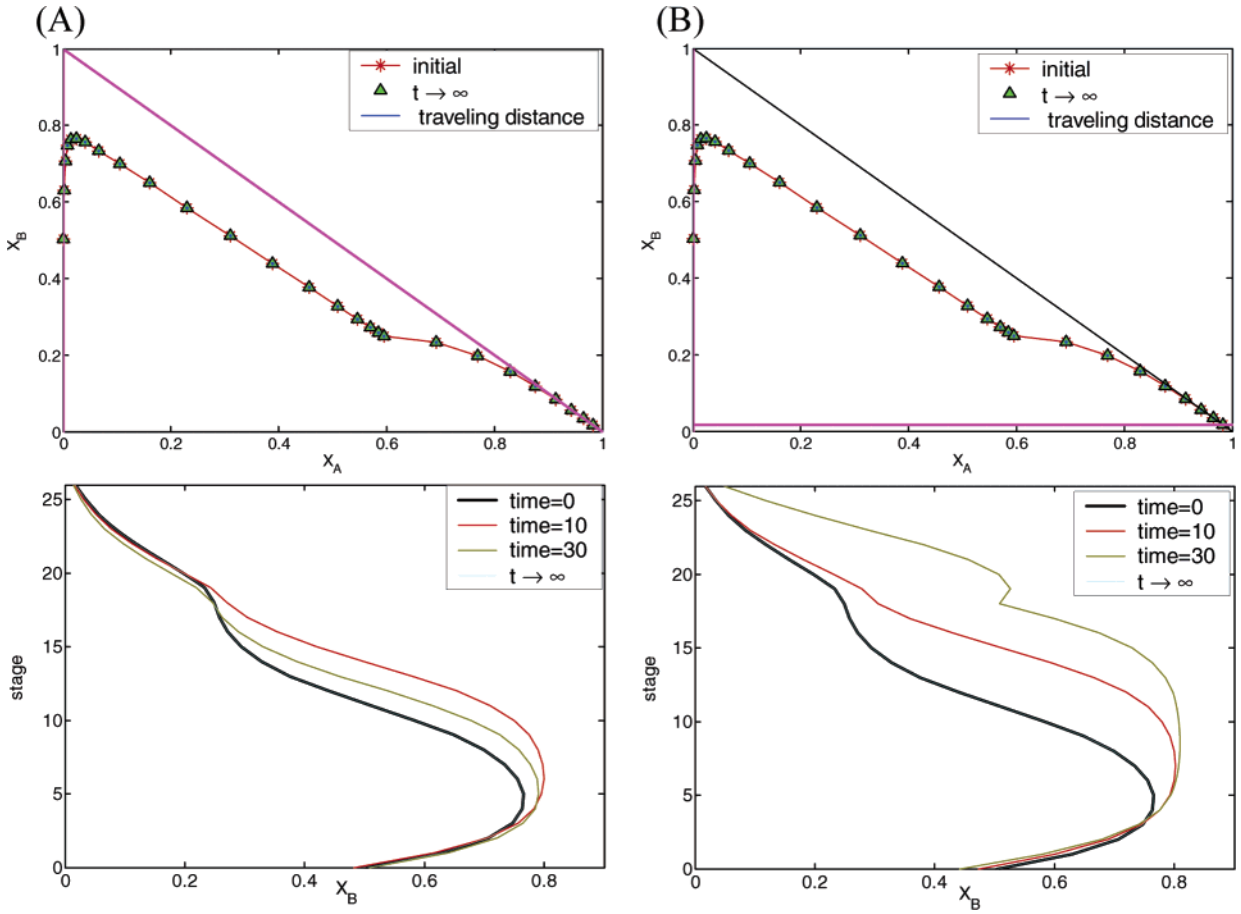


**Figure 20.** Reshaping composition profile for −20% $F$ change with (A) $x_{B,A} - x_{D,C}$ control and (B) $x_{B,A} - x_{D,B}$ control: (top) initial and final composition profiles with traveling distance (shown by arrow) and (bottom) snapshots of composition profile of B as time approaches 0, 10, 30, and ∞.

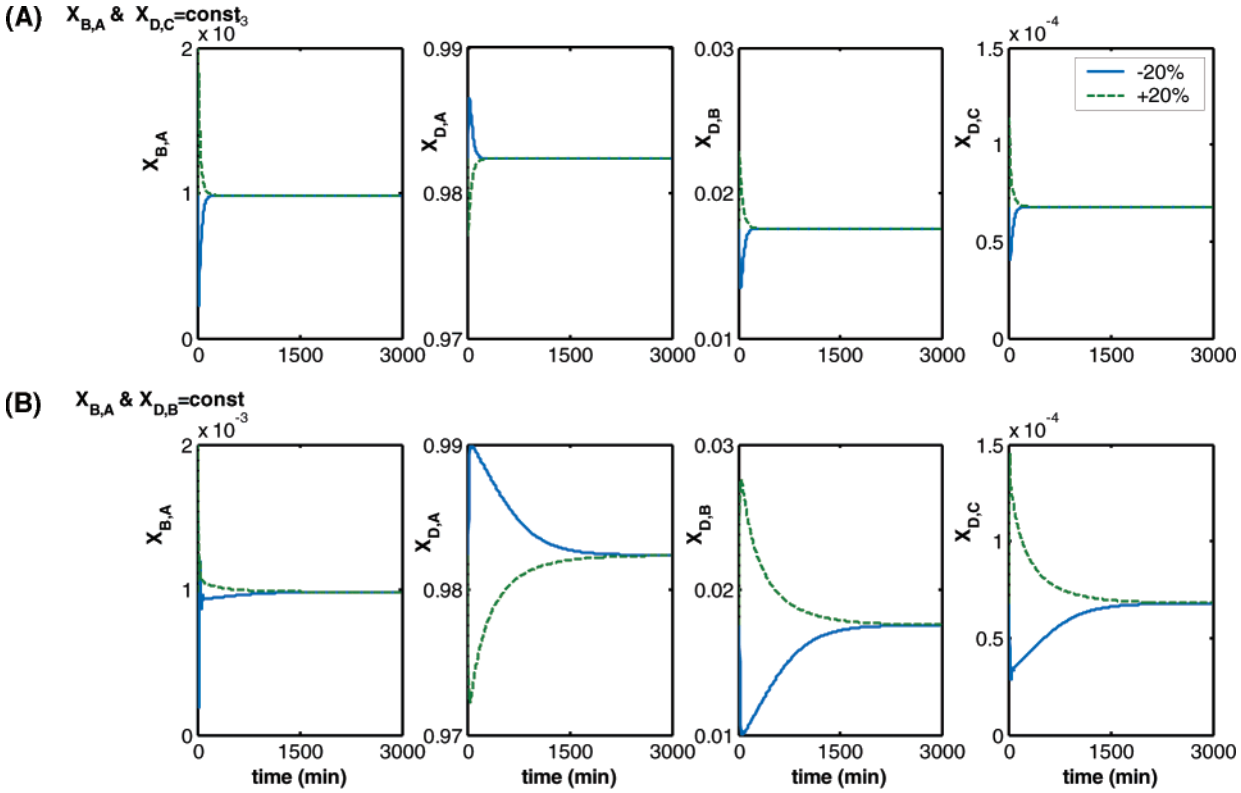


**Figure 21.** Closed-loop responses for ±20% $F$ changes with (A) $x_{B,A} - x_{D,C}$ and (B) $x_{B,A} - x_{D,B}$ control.

performance evaluation. That is, we should *eliminate* the control (temperature or composition) with a large traveling distance, but there is no guarantee that a small traveling distance leads to tight composition

responses. However, this example clearly illustrates that consistent process and control directions do help to improve composition control.

## 4. Conclusions

For ternary distillation columns, if the maximum in the intermediate boiler composition profile lies below the feed, then we want to select a temperature-control location on the "upstream" side of the peak (i.e., between the feed point and the maximum). By doing this, we stabilize the temperature and composition profiles. If we select a temperature-control point on the other side of the peak, then changes in the column feed composition will cause the intermediate boiler composition profile to wander away from its normal look in the region between the feed point and the maximum. As the intermediate component accumulates or is depleted on these trays, control of the column product composition will be poorer than when the profile is stabilized.

This phenomenon is quantified using the traveling distance that can be derived from steady-state gain matrices. It can be further explained by understanding the potential conflict between the process and control directions that govern the physical behavior in a multicomponent distillation column. Unlike the uniform control direction determined by the temperature isotherm (Figure 9), in multicomponent distillation, direct composition control allows us to choose the control direction in the top and bottom of the column (Figure 16). The quantitative measure, the traveling distance, is extended to single-end and dual-composition control to eliminate inappropriate components for control purposes. This affects the potential requirements for and benefits of an on-line composition analyzer. Then, preference is given to the control structure with consistent process and control directions. This two-step procedure is validated for single-end and dual-composition control using rigorous nonlinear simulations.

## Acknowledgment

We thank J. K. Chen and X. G. Shen for preparing some of the figures.

## Nomenclature

$A_i$ = Antoine coefficient for component $i$
$B$ = Antoine coefficient (same for all components)
$d$ = load variable representing $F$, $Z_A$, or $Z_B/Z_C$ changes
$F$ = feed flow rate
$G_{j,i}^{(k)}$ = process transfer function of component $i$ of the $j$th tray ($x_{j,i}$) under $k$th manipulated variable ($u_k$)
$G_{Lj,i}$ = load transfer function of component $i$ of the $j$th tray ($x_{j,i}$) under load variable $d$
$G_{T_j}^{(k)}$ = process transfer function of the temperature of the $j$th tray ($T_j$) under $k$th manipulated variable ($u_k$)
$G_{LT_j}$ = load transfer function of the temperature of the $j$th tray ($T_j$) under load variable $d$
$K_i$ = equilibrium constant ($K$-value) for the $i$th component
NC = number of component
NRG = nonsquare relative gain
NT = total number of trays
$P$ = pressure
$P_{i0}$ = reference vapor pressure
$P_i^{sat}$ = vapor pressure of component $i$
$T$ = temperature
$T_j$ = $j$th tray temperature
$T_0$ = reference temperature
$T_C^{sat}$ = boiling point temperature of component C at a given pressure
$u_j$ = $j$th manipulated variable
$u^{CL}$ = steady-state value of manipulated variable under perfect control
$x_i$ = liquid-phase composition of $i$th component
$x_{j,i}$ = $i$th component liquid-phase composition on $j$th tray
$y_i$ = vapor phase composition of $i$th component
$Z_i$ = feed composition of $i$th component

*Greek Symbols*

$\alpha_i$ = relative volatility of component $i$
$\Delta H$ = heat of vaporization
$\Delta x_j$ = traveling distance of tray $j$ composition

## Literature Cited

(1) Rademaker, O.; Rijnsdorp, J. E.; Maarleveld, A. *Dynamics and Control of Continuous Distillation Units*; Elsevier: New York, 1975.

(2) Buckley, P. S.; Luyben, W. L.; Shunta, J. P. *Design of Distillation Column Control Systems*; Instrument Society of America: Research Triangle Park, NC, 1985.

(3) Downs, J. J.; Moore, C. F. *Steady-State Gain Analysis for Azeotropic Distillation*. Proceedings JACC, Charlottesville, VA, 1981; Paper WP-7C.

(4) Chang, J. W.; Yu, C. C. The Relative Gain for Nonsquare Multivariable Systems. *Chem. Eng. Sci.* **1990**, *45*, 1309.

(5) Cao, Y.; Rossiter, D. An input pre-screening technique for control structure selection. *Comput. Chem. Eng.* **1997**, *21*, 563−569.

(6) Yu, C. C.; Luyben, W. L. Use of Multiple Temperatures for the Control of Multicomponent Distillation Columns. *Ind. Eng. Chem. Process Des. Dev.* **1984**, *23*, 590−597.

(7) Joseph, B.; Brosilow, C. B. Inferential Control Of Process EM DASH 1. Steady-State Analysis and Design. *AIChE J.* **1978**, *24*, 485−492.

(8) Skogestad, S.; Mejedll, T. Estimation of distillation composition from multiple temperature measurements using PLS regression. *Ind. Eng. Chem. Res.* **1991**, *30*, 2543−2555.

(9) Kano, M.; Miyazaki, K.; Hasebe, S.; Hashimoto, I. Inferential control system of distillation compositions using dynamic partial least squares regression. *J. Process Control* **2000**, *10*, 157−166.

(10) Kano, M.; Showchaiya, N.; Hasebe, S.; Hashimoto, I. .Inferential control of distillation compositions: Selection of model and control configuration. *Control Eng. Pract.* **2003**, *11*, 927−933.

(11) Pannocchia, G.; Brambilla, A. Consistency of Property Estimators in Multicomponent Distillation Control. *Ind. Eng. Chem. Res.* **2003**, *42*, 4452−4460.

(12) Luyben, M. L. Impact of Plantwide Design on Control of an Industrial Distillation Column. Presented at National Taiwan University, Taipei, Taiwan, 2002.

(13) Luyben, W. L. *Process Modeling, Simulation and Control for Chemical Engineers*, 2nd ed.; McGraw-Hill: New York, 1990.

(14) Shen, S. H.; Yu, C. C. Use of Relay-Feedback Test for Automatic Tuning of Multivariable Systems. *AIChE J.* **1994**, *40*, 627−645.

(15) Luyben, W. L. Tuning Proportional−Integral−Derivative Controllers for Integrator/Deadtime Processes. *Ind. Eng. Chem. Res.* **1996**, *35* (10), 3480−3483.

(16) Hwang, Y. L. Nonlinear Wave Theory for Dynamics of Binary Distillation Columns. *AIChE J.* **1991**, *37*, 705−723.

(17) Kienle, A. Low-order dynamic models for ideal multicomponent distillation processes using nonlinear wave propagation theory. *Chem. Eng. Sci.* **2000**, *55*, 1817−1828.

*Received for review* February 3, 2005
*Revised manuscript received* August 10, 2005
*Accepted* August 19, 2005

IE050130M